

## PAPER

[View Article Online](#)  
[View Journal](#) | [View Issue](#)

Cite this: *Polym. Chem.*, 2024, **15**,  
2377

# Fast and switchable ring-opening polymerization of biorenewable omega-substituted lactones towards sustainable copolymers with facile control over monomer sequences†

Jiayun Jiang,<sup>a</sup> Xue Liang,<sup>a</sup> Jiewen Wang,<sup>a</sup> Hongru Qiang,<sup>a</sup> Jianrui Li,<sup>a</sup>  
Jianzhong Du<sup>\*b,c</sup> and Yunqing Zhu<sup>ib,\*,a</sup>

Highly active catalysts for the ring-opening polymerization (ROP) of biorenewable monomers, especially lactones, are essential for sustainable polymers. (Thio)urea/base catalyst systems have been found to be active for unsubstituted lactones. However, while omega-substituted lactones are an important class of biorenewable monomers, the ROP of such lactones suffers from low polymerization rates, and (thio)ureas usually show low catalytic activity for omega-substituted lactones due to their high steric hindrance. Herein, fast and controlled ROPs of omega-substituted lactones, including  $\epsilon$ -decalactone ( $\epsilon$ -DL),  $\delta$ -caprolactone ( $\delta$ -CL) and  $\delta$ -decalactone ( $\delta$ -DL), were achieved using cheap and commercially available (thio)urea/base catalyst systems, whose activities were significantly improved by pairing the  $pK_a$ s of (thio)ureas with bases. (Thio)urea/IMes pairs exhibited superior activity, with the most active TU3/IMes showing turnover frequencies of 270 h<sup>-1</sup>, 996 h<sup>-1</sup> and 331 h<sup>-1</sup> in the ROP of  $\epsilon$ -DL,  $\delta$ -CL and  $\delta$ -DL, respectively. Moreover, the block, gradient and random copolymer chain sequences can be facilely modulated by different catalyst pairs during the copolymerization of  $\epsilon$ -caprolactone ( $\epsilon$ -CL) and  $\epsilon$ -DL to match different application scenarios. Therefore, this work provides fresh ideas for the transformation of similar low-activity catalysts to high-activity ones and contributes to the efficient construction of structurally and functionally diverse biorenewable polymer materials.

Received 12th April 2024,  
Accepted 18th May 2024

DOI: 10.1039/d4py00404c

[rsc.li/polymers](http://rsc.li/polymers)

## Introduction

With increasing global environmental awareness, biorenewable aliphatic polyesters have been an effective alternative to traditional petroleum-derived plastics due to their renewability, biodegradability, and biocompatibility. With these properties, they have been extensively studied for potential applications in electronics, biomedical, packaging and other fields.<sup>1–5</sup> The ring-opening polymerization (ROP) of lactones has been extensively studied as a promising method for

synthesizing aliphatic polyesters. An increasing number of new bioderived lactones are now emerging, among which omega-substituted lactones should be of particular interest. This is because the production of biorenewable lactones from hydroxy fatty acids is a commonly used process,<sup>6,7</sup> leading to the structural characteristic of many biorenewable lactones with omega substituents on the ring. Thus, it can be found that many biorenewable lactones, such as  $\delta$ -decalactone,<sup>8–10</sup>  $\delta$ -caprolactone,<sup>11–13</sup>  $\gamma$ -decalactone,  $\gamma$ -valerolactone, carvomenthide,<sup>14</sup> dihydrocarvide,<sup>14</sup> and menthine,<sup>15,16</sup> are monomers with an omega-substituted structure, and have been used for the synthesis of biorenewable polymers. These biorenewable polymers usually have low  $T_g$ , low crystallinity, good flexibility, and the potential for post-modification on the substituents.<sup>12,16–18</sup> Despite these advantages, the ring-opening polymerization of omega-substituted lactones also suffers from low polymerization rates, high reaction temperatures or rather elaborate catalysts. Therefore, achieving fast and controlled ring-opening polymerization of omega-substituted lactones is of great significance for the synthesis of functional biorenewable polyesters and deserves further research.

<sup>a</sup>Department of Polymeric Materials, School of Materials Science and Engineering, Tongji University, Shanghai 201804, China. E-mail: 1019zhuyq@tongji.edu.cn

<sup>b</sup>Department of Gynaecology and Obstetrics, Shanghai Key Laboratory of Anesthesiology and Brain Functional Modulation, Clinical Research Center for Anesthesiology and Perioperative Medicine, Translational Research Institute of Brain and Brain-Like Intelligence, Shanghai Fourth People's Hospital, School of Medicine, Tongji University, Shanghai 200434, China. E-mail: jzdu@tongji.edu.cn

<sup>c</sup>Key Laboratory of Advanced Civil Engineering Materials of Ministry of Education, School of Materials Science and Engineering, Tongji University, 4800 Caoan Road, Shanghai 201804, China

† Electronic supplementary information (ESI) available. See DOI: <https://doi.org/10.1039/d4py00404c>



In addition to exploring how to efficiently polymerize biorenewable monomers (e.g. omega-substituted lactones), achieving greener and more efficient modulation of the copolymer sequence is one of the key challenges in the field of polymer synthesis. Homopolymers or copolymers with no sequence-controlled features usually do not have structural and functional complexity. Developing simple and efficient methods for monomer sequence modulation is of great value as it could afford copolymers with block, gradient and random structures to achieve different properties.<sup>19–21</sup> For example, the main method to prepare block copolymers at present is the sequential addition of monomers, which is relatively complicated and difficult to operate compared to the emerging chemoselective copolymerization method, which can build block copolymers from a mixed monomer feedstock.<sup>19</sup> Since Coates's group reported the one-pot polymerization of epoxide, cyclic anhydride, and CO<sub>2</sub> using a single catalyst,<sup>22</sup> chemoselective polymerization has been widely studied.<sup>23–27</sup> However, it is difficult to tune the chemoselectivity of such catalytic systems to freely build random, gradient, and block copolymers according to the application scenarios. Therefore, it is necessary to develop a catalytic system that can facilitate modulate copolymer sequences to afford copolymers with structural diversity.

Currently, various catalysts have been developed for the ring-opening polymerization of lactones. Organocatalysts, including Lewis acids, phosphazene bases, *N*-heterocyclic carbenes (NHCs) and H-bond bifunctional compounds, have received the most attention since they can avoid metal residues in polyesters while still providing a high level of control over the polymerization compared to metal-based catalysts.<sup>1,3,28–30</sup> Among them, (thio)urea [(T)U], a hydrogen-bond organocatalyst, stands out for its advantages of low cost, commercial availability, and applicability in switchable polymerization.<sup>31–33</sup> Most studies have focused on the applications of (thio)urea catalysts for the ROP of unsubstituted lactones such as lactide (LA) and caprolactone (CL), which have shown high activity. However, like other types of catalysts,<sup>18,34–37</sup> (thio)ureas tend to be much less active for the ROP of omega-substituted lactones, which could be due to the large steric hindrance contributed by the substituents. This problem limits the development and transformation of bio-based omega-substituted lactones.

In Prof. Waymouth's work, it has been found that the pairing of (thio)ureas with bases of different p*K*<sub>a</sub> values greatly affects the activity of the catalyst systems for the ROP of  $\delta$ -valerolactone (VL).<sup>38</sup> However, whether this phenomenon can be generally applied to other lactones, especially to omega-substituted lactones, remains unclear, as the ROP of omega-substituted lactones is greatly affected by their substituents and is rather different from that of unsubstituted lactones. Therefore, in this work, a series of (thio)urea/base catalyst systems were carefully selected and paired to evaluate their catalytic activity in search of efficient catalysts for the ROP of omega-substituted lactones.  $\epsilon$ -Decalactone ( $\epsilon$ -DL), a biologically derived lactone that can be prepared from castor oil,<sup>36,39</sup> was first selected as the monomer for the screening of the cata-

lyst systems. To further verify the activity and trends of the efficient catalysts, the monomer scope was extended to other omega-substituted lactones, including  $\delta$ -caprolactone ( $\delta$ -CL) and  $\delta$ -decalactone ( $\delta$ -DL), which are naturally derived from coconut water and *Cryptocarya massoy*, respectively.<sup>40,41</sup> In addition, the sequence of polymer chains can be modulated by simply using different (thio)urea/base pairs in the copolymerization of  $\epsilon$ -DL and  $\epsilon$ -CL to construct block, gradient and random copolymers.

## Results and discussion

### Ring-opening polymerization of $\epsilon$ -DL using different (thio)urea/base pairs

According to previous studies, pairing (thio)ureas and bases with different p*K*<sub>a</sub> values usually leads to different catalytic mechanisms, including anionic and cooperative mechanisms, leading to varied catalytic activities.<sup>38</sup> Therefore, to explore the best catalytic system for omega-substituted lactones, a series of (thio)ureas with different substituents (Fig. 1a) combined with three organic bases (1,8-diazabicyclo[5.4.0]undec-7-ene, DBU; 2-*tert*-butylimino-2-diethylamino-1,3-dimethylperhydro-1,3,2-diazaphosphorine, BEMP; and 1,3-dimesitylimidazol-2-ylidene, IMes) (Fig. 1b) were screened for the ring-opening polymerization of  $\epsilon$ -DL, one of the commonly used bio-based omega-substituted lactones (Fig. 1c). The choice of (thio)urea/base pairs covers a wide range of p*K*<sub>a</sub> values and features both mechanisms. The p*K*<sub>a</sub> values in DMSO of (thio)ureas and bases are labelled in Fig. 1.<sup>18,42–45</sup>

All of the ROPs of  $\epsilon$ -DL were carried out in toluene with BnOH as the initiator at 25 °C and the reactions were terminated at predetermined time durations (Table 1). Instead of a high polarity solvent namely DMSO, toluene with medium polarity was selected as the solvent for the ROPs to simul-

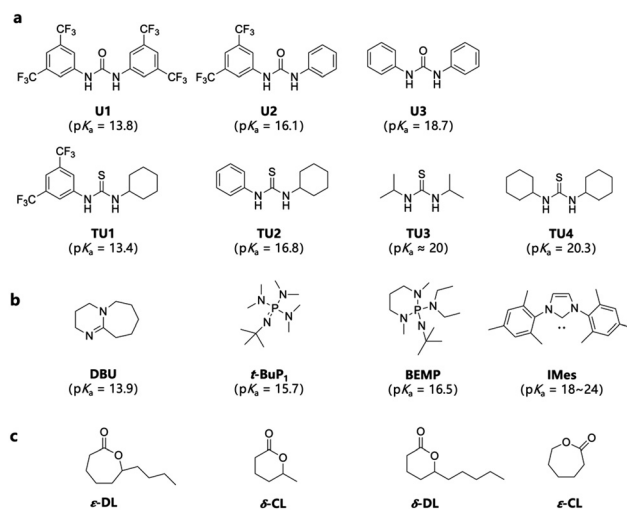


**Fig. 1** (a) Ureas and thioureas with their p*K*<sub>a</sub> values in DMSO.<sup>30,42</sup> (b) Organic bases with their p*K*<sub>a</sub> values in DMSO.<sup>43–45</sup> (c) Monomers studied.



**Table 1** Screening of (T)U/organic base catalyst systems for the ROP of  $\epsilon$ -DL<sup>a</sup>

#	(Thio)ureas	Bases	<i>t</i> (h)	Conv. <sup>b</sup> (%)	TOF <sup>c</sup> (h <sup>-1</sup> )	<i>M</i> <sub>n,theo</sub> <sup>d</sup> (kDa)	<i>M</i> <sub>n,SEC</sub> <sup>e</sup> (kDa)	<i>D</i> <sup>e</sup>
1	U1	DBU	120	18	—	—	—	—
2		BEMP	144	79	0.2	13.6	11.4	1.03
3		IMes	72	49	0.3	8.5	8.3	1.12
4	U2	DBU	120	12	—	—	—	—
5		BEMP	144	46	0.1	7.9	5.8	1.06
6		IMes	48	85	0.7	14.6	11.8	1.03
7		<i>t</i> -BuP <sub>1</sub>	48	0	—	—	—	—
8	U3	DBU	120	0	—	—	—	—
9		BEMP	120	0	—	—	—	—
10		IMes	2	86	17	14.7	10.1	1.10
11		<i>t</i> -BuP <sub>1</sub>	48	0	—	—	—	—
12	TU1	DBU	120	4	—	—	—	—
13		BEMP	120	0	—	—	—	—
14		IMes	72	24	0.1	—	—	—
15	TU2	DBU	120	0	—	—	—	—
16		BEMP	120	0	—	—	—	—
17		IMes	24	93	2	15.9	11.3	1.13
18		<i>t</i> -BuP <sub>1</sub>	48	0	—	—	—	—
19	TU3	DBU	120	0	—	—	—	—
20		BEMP	120	0	—	—	—	—
21		IMes	8 min	90	270	15.4	11.3	1.20
22		<i>t</i> -BuP <sub>1</sub>	48	0	—	—	—	—
23	TU4	IMes	3	92	12	15.7	10.3	1.15

<sup>a</sup> Polymerizations were performed in dry toluene at 25 °C with  $[\epsilon\text{-DL}]_0 = 5 \text{ M}$ ;  $[\epsilon\text{-DL}]/[(\text{T})\text{U}]/[\text{base}]/[\text{I}] = 100/2.5/2.5/1$ ;  $\text{I} = \text{BnOH}$ . <sup>b</sup> Monomer conversion determined by <sup>1</sup>H NMR in CDCl<sub>3</sub> using integrals of the characteristic signals. <sup>c</sup> Turnover frequency (TOF) = mole of the consumed monomer/mole of the (thio)urea catalyst per hour. <sup>d</sup>  $M_{n,theo} = M_{(\epsilon\text{-DL})} \times ([\epsilon\text{-DL}]_0/[I]_0) \times \text{conv.} + M_{(\text{BnOH})}$ . <sup>e</sup> Determined by SEC in THF at a flow rate of 1.0 mL min<sup>-1</sup> at 40 °C, calibrated with polystyrene standards.

taneously ensure the occurrence of different catalytic mechanisms and maintain good control over the polymerization process.<sup>46</sup> The <sup>1</sup>H NMR spectrum for the ROP of  $\epsilon$ -DL is shown in Fig. S1.† All the polymers displayed unimodal SEC traces with narrow distributions (Fig. S2†). Significant differences in the catalytic effects of different catalyst systems can be observed in the ROP of  $\epsilon$ -DL. For the weakest DBU, no considerable conversion of  $\epsilon$ -DL was observed in combination with either urea or thiourea, even when the reaction time was extended to 120 h. U1 and TU1, with *pK<sub>a</sub>* values close to that of DBU, can lead to 18% and 4% conversion of  $\epsilon$ -DL, respectively. This could be due to the high activity in the ‘matching’ case, where the highest catalytic activity of (thio)urea/base catalyst systems towards lactide and unsubstituted lactones was usually observed when the *pK<sub>a</sub>* value of the (thio)urea closely matched that of the protonated base.<sup>38</sup> This could be the result of the competition between two mechanisms, the anionic mechanism and the cooperation mechanism, since in the ‘matching’ case, the deprotonation of (thio)urea by the base and the formation of a hydrogen-bonded complex with the base will proceed simultaneously, leading to equilibrium.<sup>47,48</sup>

When DBU is not strong enough to deprotonate the (thio)urea, *i.e.* when its *pK<sub>a</sub>* value is relatively smaller, the polymerization is dominated by the cooperative mechanism. In this case, almost all combinations involved with DBU resulted in failed polymerization. Similarly, when pairing the moderate BEMP with (thio)ureas of greater *pK<sub>a</sub>* values (Table 1, entries 9 and 20), none of the cases of the cooperative mechanism can

lead to the ROP of  $\epsilon$ -DL. This is in contrast to the results of previous studies involving lactide and unsubstituted lactones,<sup>38</sup> as all catalyst systems featuring the cooperative mechanism (Table 1, entries 4, 8, 9, 15, 19 and 20) led to failures in the ROP of  $\epsilon$ -DL. In addition, *N'*-*tert*-butyl-*N,N,N',N'',N''*-hexamethylphosphorimidic triamide (*t*-BuP<sub>1</sub>) with a *pK<sub>a</sub>* value of 15.7 was selected in combination with U2, U3, TU2, and TU3 (*pK<sub>a</sub>* > 16.1), respectively, to further validate the low activity of the cooperative mechanism towards omega-substituted lactones (Table 1, entries 7, 11, 18 and 22). Consistent with the results of DBU and BEMP, none of these catalyst pairs of the cooperative mechanism could initiate the ring-opening polymerization of  $\epsilon$ -DL, suggesting that the cooperative mechanism may not work for omega-substituted lactones. This may be due to the following reasons: first, the hydroxyl group at the propagating chain end formed by the ROP of omega-substituted lactones is a secondary alcohol. It has been noted that secondary alcohols are less reactive than primary alcohols,<sup>49,50</sup> making it more difficult to activate secondary alcohols at the propagating chain end. In addition, compared to the anionic mechanism in which the activations of the propagating chain end and the monomer occur on the same (thio)urea molecule, the nucleophilic attack on the monomer in the cooperative mechanism would be more difficult due to the steric hindrance of the substituents.

BEMP led to successful polymerization only in combination with U1 and U2. It is noteworthy that, in contrast to the previous findings, BEMP/U1 (anionic mechanism) showed higher activity than BEMP/U2 (‘matching’ mechanism) in the ROP of



$\epsilon$ -DL. As it is out of the scope of this work, this unusual phenomenon will be investigated in the future. In contrast, TU1 and TU2, which have similar  $pK_a$  values, did not initiate the ROP of  $\epsilon$ -DL. Similarly, when combined with DBU, U1 and U2 also showed better activity than TU1 and TU2. This could be due to the fact that ureas are stronger hydrogen bond donors than thioureas of similar acidity, which has also been reported by Kozłowski.<sup>46,51,52</sup> In addition, the urea anion is a stronger base than the thiourea anion due to the large sulfur atom that increased the stability of the conjugate base.

When the strongest IMes was used,  $\epsilon$ -DL ROP occurred in all cases. The activity of the catalyst systems reached its maximum in the 'matching' case, as the TOF value of TU3/IMes was as high as  $270\text{ h}^{-1}$ . In contrast to the observations about U1/TU1 and U2/TU2, TU3 exhibited higher activity than U3 in the ROP of  $\epsilon$ -DL when combined with IMes. It is hypothesized that this unusual phenomenon could be due to the steric hindrance since the nitrogen atom of TU3 is bonded to an isopropyl group, instead of a bulky benzene ring of U3. This steric hindrance effect may not be profound in the ROP of unsubstituted lactones but could pose a significant impact on the ROP of omega-substituted lactones due to their large

substituents. To verify this hypothesis, another thiourea, TU4, with higher steric hindrance but almost identical  $pK_a$  to TU3, was employed to pair with IMes for  $\epsilon$ -DL ROP (Table 1, entry 23). The TOF value of TU4/IMes was found to be  $12\text{ h}^{-1}$ , which is much lower than that of TU3/IMes. This indicates that steric hindrance indeed has a great impact on the (thio)urea/base catalyzed ROP of substituted lactones. Low steric hindrance of the (thio)ureas facilitates the simultaneous activation of the propagating chain end and the monomer on the same (thio)urea molecule, leading to efficient nucleophilic attack.

Due to the particularly high activity of TU3/IMes, the reaction rate is too high for aliquoting and monitoring, as the monomer was almost completely consumed as soon as the reaction mixture was prepared in a glove box. Therefore, entry 6 was chosen as the model reaction for kinetic studies due to its moderate activity. As shown in Fig. 2a and b, the linear increase in molecular weight with monomer conversion indicates the characteristics of controlled living polymerization. However, the SEC traces in Fig. 2b are not perfectly symmetrical, showing a slight 'tail' at a shorter retention time due to initiation from a trace amount of water present in the monomers. This phenomenon has been discussed in detail in pre-

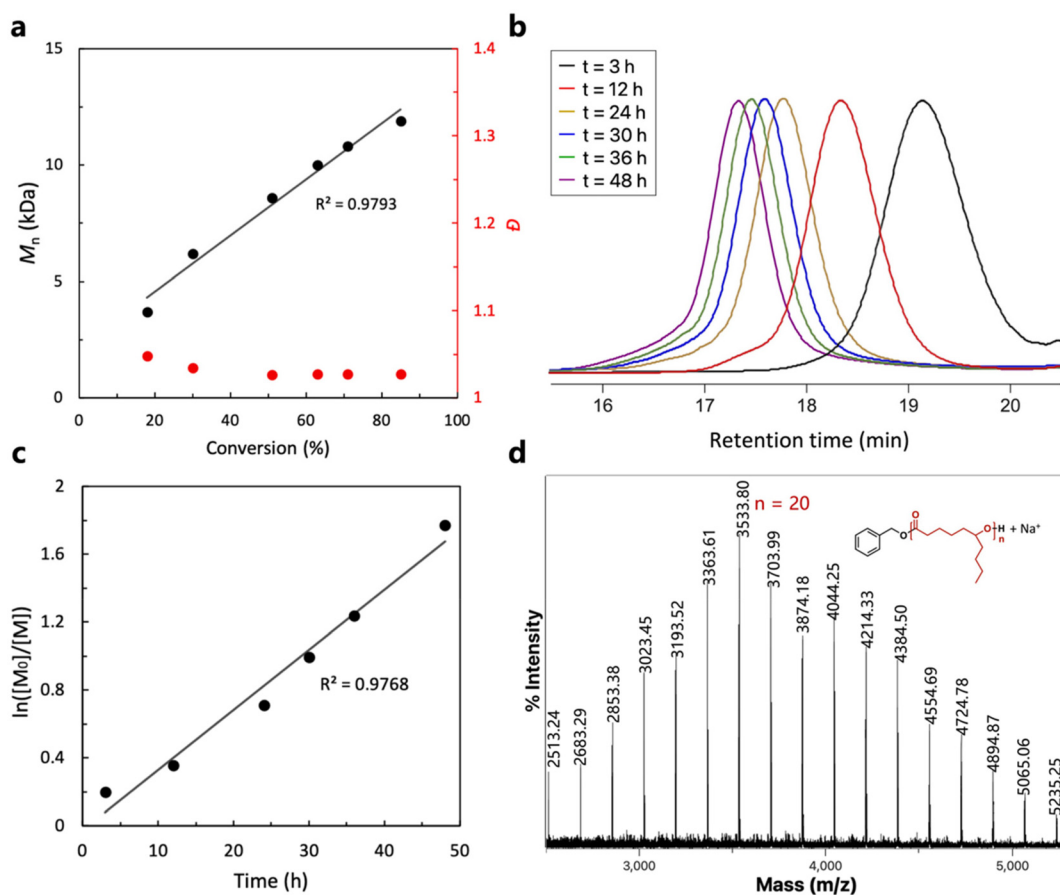


**Fig. 2** (a)  $M_{n,SEC}$  and dispersity ( $\bar{D}$ ) vs. monomer conversion, (b) typical SEC curves of aliquots taken at different time intervals during the ROP of  $\epsilon$ -DL, (c) semi-logarithmic plot of monomer concentration over time and (d) the MALDI-TOF mass spectrum of P( $\epsilon$ -DL) produced with U2/IMes as the catalyst ( $M_n = 6.0\text{ kDa}$ ,  $\bar{D} = 1.04$ , Table 1, entry 6).





vious works by other groups.<sup>29,53</sup> Furthermore, semi-logarithmic plot analysis demonstrated the first-order feature, which is also consistent with the living polymerization features (Fig. 2c). A chain extension experiment was later performed to further confirm the living features of the ROP of  $\epsilon$ -DL mediated by the (thio)urea/base catalyst systems. After 100 equivalents of  $\epsilon$ -DL were completely converted, another 100 equivalents of  $\epsilon$ -DL were added to the reaction mixture. The SEC traces in Fig. S3† demonstrate an increase in the molecular weight of the polymer from 13.6 kDa to 25.7 kDa that occurred after the sequential addition of monomers while still maintaining a narrow molecular weight distribution (<1.08).

(Thio)urea catalysts have previously been found to initiate polymer chains, making it difficult to predict molecular weights from the amount of initiator, compromising the controllable nature of living polymerization.<sup>34</sup> Therefore, in order to further identify the polymer structure and initiation mechanism, the matrix-assisted laser desorption/ionization time-of-flight mass spectrometry (MALDI-TOF MS) technique was used to analyze the structure of the obtained P( $\epsilon$ -DL). The MALDI-TOF mass spectrum reveals only one series of molecular ion peaks with an interval of *ca.* 170.13 Da, corresponding to the exact molar mass of the  $\epsilon$ -DL repeat unit (Fig. 2d). The molar mass  $M = n \times 170.13 (M_{DL}) + 108.14 (M_{BnOH}) + 22.99 (M_{Na+})$  of each peak corresponds to linear P( $\epsilon$ -DL) chains initiated solely by BnOH and terminated by the hydroxyl group, which is also consistent with the results of the <sup>1</sup>H NMR spectrum (Fig. S1†), suggesting that the catalyst system does not initiate polymer chains and has excellent control over the molecular weight and structure of the polymer. The chain structure of the polymer catalyzed by U2/BEMP was also characterized by MALDI-TOF (Fig. S4†) and the results are also in agreement with the previous ones.

The conversions at different times during the ROP of  $\epsilon$ -DL by different catalyst systems were plotted into graphs (Fig. S5†), followed by the discussion on the activity trends and reaction mechanisms for different catalyst pairs. In conclusion, in the ROP of  $\epsilon$ -DL, the (thio)urea/IMes pairs exhibited superior activity in all catalyst systems. In particular, TU3/IMes was used for the ROP of  $\epsilon$ -DL at room temperature with a TOF value of 270 h<sup>-1</sup>, exhibiting activity far exceeding that of any other catalysts at the same or higher polymerization temperatures (Fig. S6†).<sup>18,34,36</sup>

### Ring-opening polymerization of other omega-substituted lactones using different (thio)urea/IMes pairs

In the screening of the (thio)urea/base catalytic system carried out in the ROP of  $\epsilon$ -DL, the (thio)urea/IMes catalyst pairs showed high activity superior to the other groups. To further verify the high activity and activity trends of the (thio)urea/IMes catalyst pairs by a wider range of omega-substituted lactones, these catalyst systems were subsequently used for the ring-opening polymerization of  $\delta$ -CL and  $\delta$ -DL (Tables S1 and S2†). The <sup>1</sup>H NMR spectra for the ROP of  $\delta$ -CL and  $\delta$ -DL are shown in Fig. S7 and S8.†

The (thio)urea/IMes catalyst systems showed particularly high activity when screened by the ring-opening polymerization of  $\delta$ -CL (Table S1†), compared to the performance in the ROP of  $\epsilon$ -DL under the same conditions. All (thio)urea/IMes systems had much higher TOF values in the ROP of  $\delta$ -CL than  $\epsilon$ -DL. This difference may be due to the greater steric hindrance of the substitution of  $\epsilon$ -DL, which confines its polymerization rate. This can be further confirmed by the results of the ring-opening polymerization of  $\delta$ -DL catalyzed by (thio)urea/IMes (Table S2†). The TOF values in the ROP of  $\delta$ -DL were smaller than those observed in the ROP of  $\delta$ -CL, which can be attributed to the substitution of the *n*-amyl group on the ring. Moreover, SEC analyses of polymers obtained by the ROPs of  $\delta$ -CL and  $\delta$ -DL mediated by (thio)urea/IMes all exhibited monomodal curves and narrow molecular weight distributions, confirming that the polymerization remains highly controlled (Fig. S9 and S10†). The living behaviour of the polymerization of  $\delta$ -CL and  $\delta$ -DL is subsequently demonstrated by the first-order features shown by the plots of  $\ln([M]_0 - [M]_{eq})/([M]_t - [M]_{eq})$  vs. time, the linear increase in molecular weight with conversion and the consistently low molecular weight distribution (Fig. 3). Here, neither the polymerization of  $\delta$ -CL nor that of  $\delta$ -DL can achieve a conversion greater than 90%, which is probably caused by the equilibrium of the monomer and the polymer in the reaction system. As the thermodynamic driving force for the polymerization of cyclic monomers is closely related to ring size, relatively low equilibrium conversion is commonly observed in the polymerization of six-membered lactones with low ring strain.<sup>54</sup> Additionally, some reports indicated that the equilibrium conversion of substituted  $\delta$ -lactones decreases with larger substituents on the ring,<sup>55</sup> which is consistent with the observation that the equilibrium conversion of  $\delta$ -DL (*ca.* 70%) is generally lower than that of  $\delta$ -CL (*ca.* 80%) under the same conditions.

The process of the ring-opening polymerization of  $\delta$ -CL and  $\delta$ -DL using the (thio)urea/IMes catalyst systems was sampled for monitoring and the results are presented in plots to visualize the trends in activity (Fig. 3a and c). The activity trends of the (thio)urea/IMes catalyst systems are consistent with the previous findings in  $\epsilon$ -DL ROP. All the activities increased with decreasing acidity of the urea or thiourea, which corresponds to the shift from the anionic mechanism to the 'matching' mechanism. In the ring-opening polymerizations of  $\delta$ -CL and  $\delta$ -DL, considerable monomer conversion could be achieved in minutes using IMes and TU3/U3. In particular, the TOF values of TU3/IMes in the ROP of  $\delta$ -CL and  $\delta$ -DL were as high as 996 h<sup>-1</sup> and 331 h<sup>-1</sup>, respectively, which were much higher than those of the catalysts (*e.g.* DPP and TBD) commonly used in the ROP of  $\delta$ -CL and  $\delta$ -DL at room temperature (Fig. S11†).<sup>9,13,56,57</sup> Although the TOF values of a strontium catalyst (TOF = 360 h<sup>-1</sup> and 228 h<sup>-1</sup> for  $\delta$ -CL and  $\delta$ -DL, respectively) are reluctantly close to our system, its application may still be limited by the high cost, pyrophoric feature, and concerns regarding the toxicity of metal residues in polymers. Therefore, the higher activity exhibited by (thio)urea/IMes in the ROP of  $\delta$ -CL and  $\delta$ -DL further verified that the anionic and



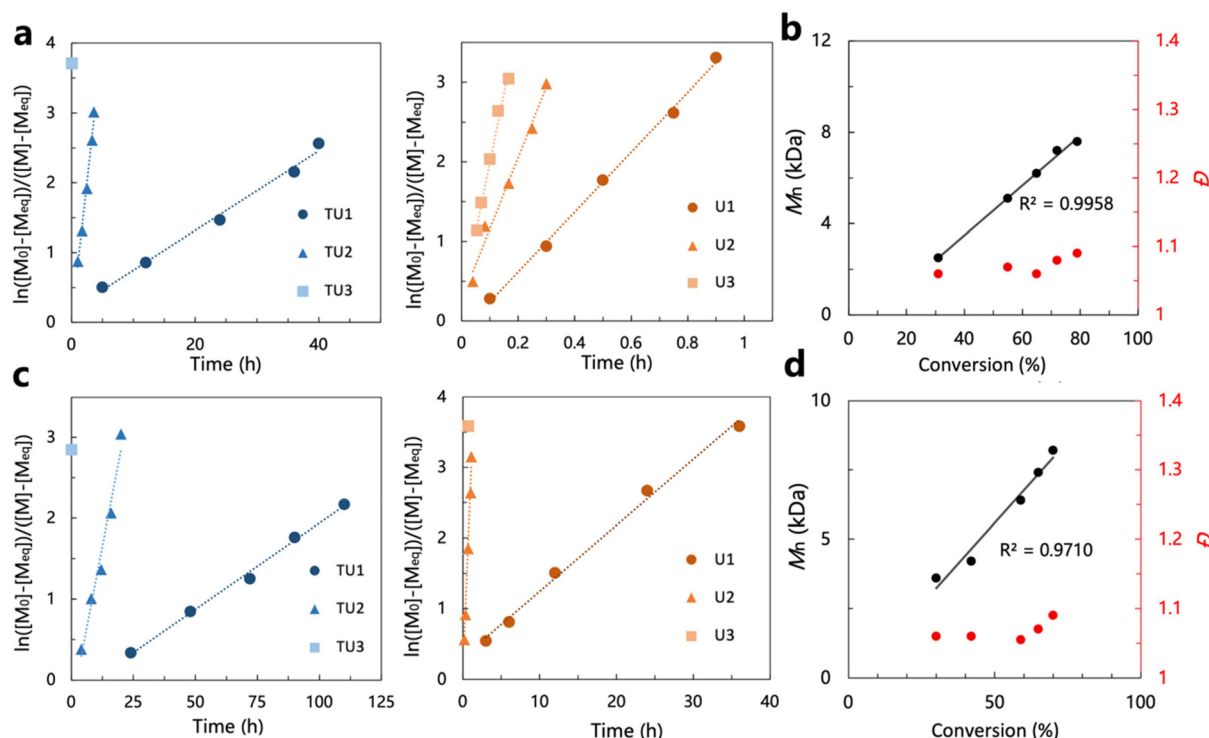


**Fig. 3** (a) Kinetic plots of  $\ln([M]_0 - [M]_{eq})/([M]_t - [M]_{eq})$  vs. time for the ROP of  $\delta$ -CL and (b)  $M_{n,SEC}$  and dispersity ( $\bar{D}$ ) vs. monomer conversion (U2/IMes), (c) kinetic plots of  $\ln([M]_0 - [M]_{eq})/([M]_t - [M]_{eq})$  vs. time for the ROP of  $\delta$ -DL and (d)  $M_{n,SEC}$  and dispersity ( $\bar{D}$ ) vs. monomer conversion (U2/IMes).

'matching' mechanisms are more applicable to omega-substituted lactones.

#### Ring-opening copolymerization of $\epsilon$ -DL and $\epsilon$ -CL using (thio)urea/IMes pairs

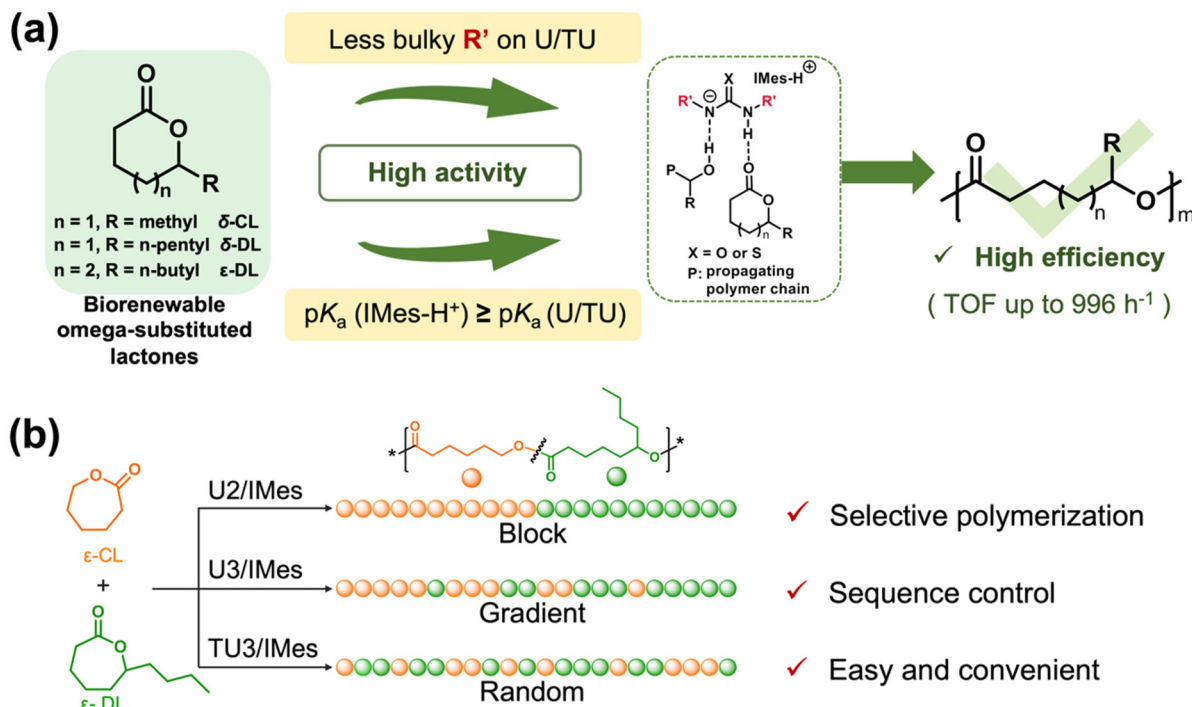
From the previous experimental results, it is clear that the (thio)urea/base catalyst systems are much more active for lactones with smaller side chains, such as  $\delta$ -CL. Hence, given the reactivity difference of these catalyst systems in the homopolymerization of different monomers, it may be possible to achieve well-defined polymer sequences by the ROPs of lactone mixtures in one pot. We believe that the modulation of the copolymer structure may be achieved by selecting catalyst systems with different activities for the synthesis of random, gradient and block copolymers (Scheme 1b). To ensure a high reactivity difference, unsubstituted lactone  $\epsilon$ -caprolactone ( $\epsilon$ -CL) was chosen as the comonomer for copolymerization with  $\epsilon$ -DL (Table 2). Although  $\epsilon$ -CL is usually prepared industrially from petrol, more and more studies are now focused on developing green and efficient methods for the preparation of  $\epsilon$ -CL,<sup>58</sup> which makes it potentially sustainable. U2/IMes, which exhibits moderate activity in the homopolymerization of  $\epsilon$ -DL, was first selected as the catalyst for copolymerization with  $\epsilon$ -CL (Table 2, entry 1). The copolymerization was monitored by  $^1\text{H}$  NMR spectroscopy (Fig. S12 and S13†). Due to the high activity of U2/IMes towards  $\epsilon$ -CL,  $\epsilon$ -CL reached complete conversion within 30 min, followed by the ROP of  $\epsilon$ -DL to produce an  $\epsilon$ -CL/ $\epsilon$ -DL copolymer. The SEC curve of the copolymer

(Fig. S14†) showed a monomodal distribution and the molecular weight also matched the theoretical values ( $M_n = 16.6$  kDa,  $\bar{D} = 1.32$ ), indicating that the copolymerization process is highly controlled.

To further confirm the selectivity of U2/IMes for  $\epsilon$ -CL and  $\epsilon$ -DL, the copolymerization of  $\epsilon$ -CL/ $\epsilon$ -DL by U2/IMes was also monitored using *in situ* IR spectroscopy (Fig. 4a). The FTIR spectra of  $\epsilon$ -DL and  $\epsilon$ -CL monomers are shown in Fig. S15† to justify the choice of bands for monitoring. It was found that  $\epsilon$ -CL ROP occurred first, as evidenced by the decrease in the resonance attributed to  $\epsilon$ -CL at  $1051\text{ cm}^{-1}$ . During this period,  $\epsilon$ -DL did not undergo any conversion, as the corresponding resonance at  $1530\text{ cm}^{-1}$  hardly decreased. A reduction of the resonance assigned to  $\epsilon$ -DL was only observed after the complete consumption of  $\epsilon$ -CL. This suggests that U2/IMes preferentially catalyzes the ROP of  $\epsilon$ -CL and switches to the ROP of  $\epsilon$ -DL once  $\epsilon$ -CL is completely consumed. Therefore, the copolymerization of  $\epsilon$ -CL and  $\epsilon$ -DL by the U2/IMes catalytic system affords copolymers with a block structure.

Alternatively, the more reactive U3/IMes and the most reactive TU3/IMes were selected for the copolymerization of  $\epsilon$ -CL and  $\epsilon$ -DL. The monomers were able to reach considerable conversion ( $> 80\%$ ) within a few hours and copolymers with the corresponding molecular weights and narrow molecular weight distributions were synthesized (Table 2, entries 2–4). The ring-opening copolymerization of  $\epsilon$ -CL and  $\epsilon$ -DL mediated by U3/IMes and TU3/IMes was also monitored by *in situ* IR spectroscopy. For U3/IMes, the conversion of  $\epsilon$ -DL occurred





**Scheme 1** (a) Fast and efficient ring-opening polymerization of biorenewable omega-substituted lactones catalyzed by (thio)urea/base catalyst systems and (b) copolymerization of  $\varepsilon\text{-DL}$  and  $\varepsilon\text{-CL}$  to produce block, gradient and random copolymers using different (T)U/base catalyst systems.

**Table 2** Copolymerization of  $\varepsilon\text{-DL}$  and  $\varepsilon\text{-CL}$  catalyzed by (T)U/base catalyst systems<sup>a</sup>

Entry	Catalyst (s)	$[\varepsilon\text{-CL}]/[\varepsilon\text{-DL}]$	$t$ (h)	Conv. $\varepsilon\text{-CL}^b$ (%)	Conv. $\varepsilon\text{-DL}^b$ (%)	$M_{n,\text{theo}}^c$ (kDa)	$M_{n,\text{SEC}}^d$ (kDa)	$D^d$	Dyad <sup>e</sup>			
									CL*-CL	CL*-DL	DL*-CL	DL*-DL
1	U2/IMes	100/100	102	99	75	23.3	16.6	1.32	0.46	0.08	0.02	0.44
2	U3/IMes	100/100	4	99	86	26.0	22.1	1.33	0.39	0.12	0.09	0.40
3	U3/IMes	50/100	3	99	93	21.6	19.3	1.30	0.20	0.10	0.09	0.61
4	TU3/IMes	100/100	40 min	99	92	27.1	28.8	1.35	0.31	0.20	0.19	0.30

<sup>a</sup> Polymerizations were performed in dry toluene at 25 °C with  $[\varepsilon\text{-CL}]_0 = 2.5 \text{ M}$ ;  $[(\text{T})\text{U}]/[\text{base}]/[\text{I}] = 2.5/2.5/1$ ;  $\text{I} = \text{BnOH}$ . <sup>b</sup> Monomer conversion determined by  $^1\text{H}$  NMR in  $\text{CDCl}_3$  using integrals of the characteristic signals. <sup>c</sup>  $M_{n,\text{theo}} = M_{(\varepsilon\text{-CL})} \times ([\varepsilon\text{-CL}]_0/[\text{I}]_0) \times \text{conv.} + M_{(\varepsilon\text{-DL})} \times ([\varepsilon\text{-DL}]_0/[\text{I}]_0) \times \text{conv.} + M_{(\text{BnOH})}$ . <sup>d</sup> Determined by SEC in THF at a flow rate of  $1.0 \text{ mL min}^{-1}$  at 40 °C, calibrated with polystyrene standards. <sup>e</sup> Determined by quantitative  $^{13}\text{C}$  NMR spectroscopy, with \* defining the carbonyl analyzed.

before the complete conversion of  $\varepsilon\text{-CL}$ , suggesting that a gradient copolymer structure was most likely formed (Fig. 4b). For TU3/IMes, a simultaneous decrease in the resonances attributed to  $\varepsilon\text{-CL}$  and  $\varepsilon\text{-DL}$  at  $1051 \text{ cm}^{-1}$  and  $1530 \text{ cm}^{-1}$  can be clearly observed, respectively. This suggests a mutual propagation of  $\varepsilon\text{-DL}$  and  $\varepsilon\text{-CL}$ , leading to the formation of a random copolymer (Fig. 4c). Besides,  $^1\text{H}$  DOSY NMR spectra of copolymers prepared by U2/IMes, U3/IMes and TU3/IMes all show a single diffusion coefficient, which confirms the formation of  $\varepsilon\text{-CL}/\varepsilon\text{-DL}$  copolymers (Fig. S16, S17 and S18†).

To verify the chain sequence, all  $\varepsilon\text{-CL}/\varepsilon\text{-DL}$  copolymers were analyzed by quantitative  $^{13}\text{C}$  NMR spectroscopy, and the carbonyl region was analyzed and integrated to reveal the chain structure (Fig. 5). The sequence of two (different) adjacent monomers in a polymer is characterized by the carbonyl dyad

resonance. The carbonyl dyad resonance corresponding to an  $\varepsilon\text{-CL}$  carbonyl adjacent to an  $\varepsilon\text{-CL}$  repeat unit (CL\*-CL, where the asterisk represents the observed carbonyl) can be observed at  $\delta = 173.6 \text{ ppm}$ , while the smaller shoulder peak on the left corresponds to the carbonyl dyad resonance of CL\*-DL. Similarly, the three split peaks of the carbonyl dyad resonance observed at  $\delta = 173.4 \text{ ppm}$  can be attributed to DL\*-DL and DL\*-CL resonances, respectively. For copolymers produced by U2/IMes, the integration of the CL\*-DL (0.08) and DL\*-CL (0.02) resonances is particularly smaller than those of DL\*-DL (0.44) and CL\*-CL (0.46), indicating the high selectivity of U2/IMes and the block-like polymer chain sequence. Notably, some transesterification may occur due to the relatively long reaction time of entry 1, which could account for the presence of some CL\*-DL and DL\*-CL carbonyl dyad resonances.



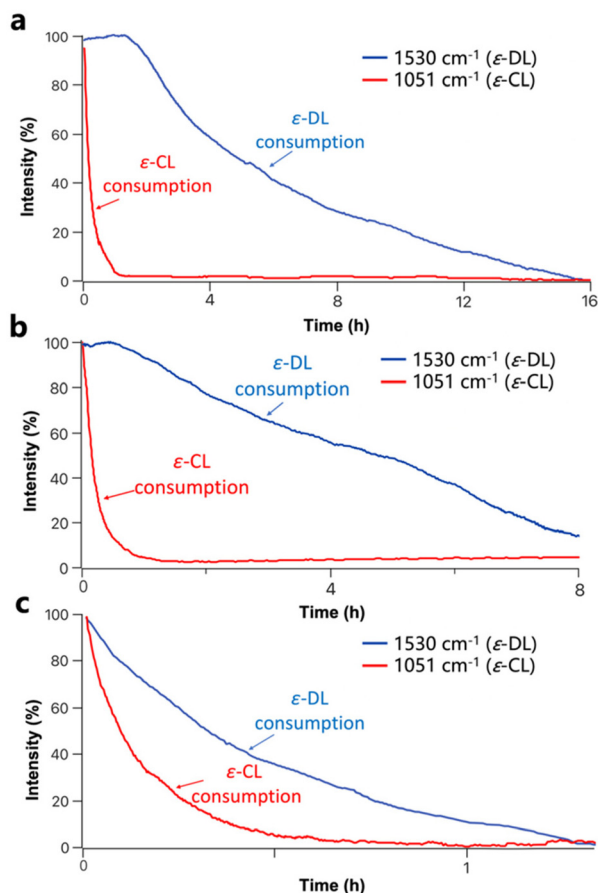


Fig. 4 Formation of the  $\epsilon$ -CL/ $\epsilon$ -DL copolymer produced by (a) U2/IMes, (b) U3/IMes and (c) TU3/IMes monitored by *in situ* IR spectroscopy.

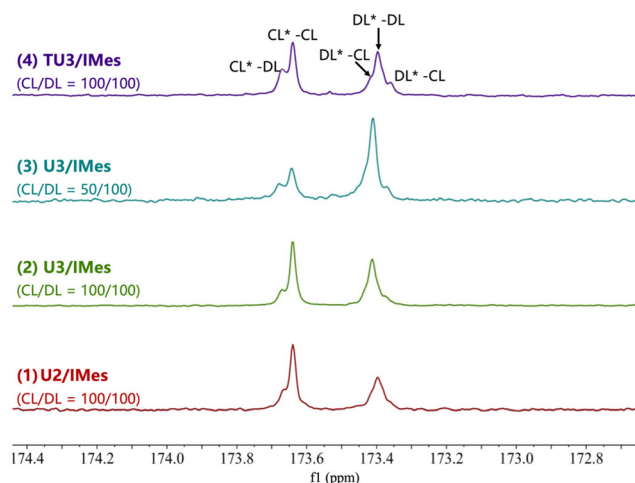


Fig. 5 Quantitative  $^{13}\text{C}$  NMR spectra of the carbonyl region of the  $\epsilon$ -DL/ $\epsilon$ -CL copolymer (125 MHz,  $\text{CDCl}_3$ , 298 K).

When the U3/IMes with moderate activity was used, there was an increase in the integrals of the  $\text{CL}^*\text{-DL}$  (from 0.08 to 0.12) and  $\text{DL}^*\text{-CL}$  (from 0.02 to 0.09) resonances, but still

much less than those of the  $\text{DL}^*\text{-DL}$  and  $\text{CL}^*\text{-CL}$  resonances. This phenomenon indicates that the selectivity for  $\epsilon$ -CL and  $\epsilon$ -DL is reduced in the U3/IMes system, thus favouring the formation of copolymers with a potential gradient structure. For comparison, the monomer ratio of  $\epsilon$ -CL/ $\epsilon$ -DL was then reduced to 50/100 with U3/IMes (Table 2, entry 3). The result of  $^{13}\text{C}$  NMR shows that the integrals of the major  $\text{DL}^*\text{-DL}$  and  $\text{CL}^*\text{-CL}$  dyad resonances in the carbonyl region of the copolymer have also changed to match the initial monomer feed ratio. There is a slight decrease in the integral of the  $\text{CL}^*\text{-DL}$  resonance in the copolymer from 0.12 to 0.10 as the content of  $\epsilon$ -CL decreases, suggesting a reduction of the gradation length in the copolymer. When it comes to the most active TU3/IMes, the relative integrals obtained by deconvolution of the carbonyl resonances corresponding to  $\text{CL}^*\text{-DL}$  and  $\text{CL}^*\text{-CL}$  became closer (0.20 vs. 0.31), indicating that a random copolymer was likely to be produced. This may be due to the very high activity of TU3/IMes that the reactivity difference between  $\epsilon$ -CL and  $\epsilon$ -DL became smaller, making the  $\epsilon$ -DL monomer getting inserted into the polymer chain at a similar rate to that of  $\epsilon$ -CL. It can also be evidenced by the fact that the least active U2/IMes has the highest selectivity for the copolymerization of monomer mixtures. Therefore, by simply changing the combination of (thio)ureas and bases, copolyesters with different structures (*e.g.* block, gradient and random structures) can be facilely and efficiently prepared in one-pot from a mixed monomer feedstock.

The thermal properties of the copolymers were investigated by DSC analysis to demonstrate the effect of block, gradient and random structures on thermal properties. In Fig. 6, the copolymer prepared from U2/IMes exhibits a glass transition temperature ( $T_g$ ) of  $-56^\circ\text{C}$ , which is between that of the two homopolymers [ $-53$  and  $-60^\circ\text{C}$  for  $\text{P}(\epsilon\text{-DL})$  and  $\text{P}(\epsilon\text{-CL})$ , respectively], and a  $T_m$  at  $41^\circ\text{C}$ , which can be assigned to the

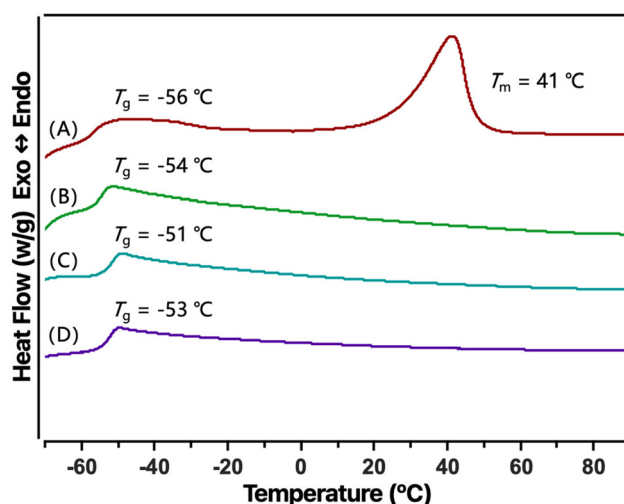


Fig. 6 DSC thermograms for  $\text{P}(\epsilon\text{-CL-co-}\epsilon\text{-DL})$  produced by different catalyst systems: (A) U2/IMes (Table 2, entry 1), (B) U3/IMes (Table 2, entry 2), (C) U3/IMes (Table 2, entry 3), and (D) TU3/IMes (Table 2, entry 4).





semi-crystalline PCL block. This suggests that the block structure of the copolymer is favourable for generating phase separation. This observation further evidenced the successful production of block copolymers by U2/IMes through its excellent selectivity. In contrast, the copolymers obtained from U3/IMes and TU3/IMes all showed only one  $T_g$  without melting transition, which corresponded to the gradient and random structures due to reduced selectivity. Furthermore, the disappearance of  $T_m$  indicates that the crystallinity of PCL can be simply and effectively reduced by the choice of catalyst pairs. This indicates that by simply changing the combination of catalyst pairs, the crystallinity of copolyesters can be easily tuned. These results confirmed the synthesis of polymers with different chain structures by selecting catalyst systems with different activities. This is of great value in terms of modulating the polymer chain sequence, which can further modulate its properties to match different application scenarios.

## Conclusions

In summary, a series of biorenewable omega-substituted lactones were successfully polymerized using inexpensive and readily commercially available catalysts and co-catalysts. The polymerization process is highly controlled and exhibits living features. The (thio)urea/base systems produce polymers with very narrow molecular weight distributions ( $<1.10$  in most cases). The most active TU3/IMes demonstrated a TOF value of up to  $270\text{ h}^{-1}$  in the ROP of  $\epsilon$ -DL, far exceeding those of the previously reported catalysts, including TBD,  $\text{Sn}(\text{Oct})_2$ , zinc complex, *etc.* This indicates that for the (thio)urea/IMes catalytic pairs, the 'matching' mechanism features higher activity for the ROP of omega-substituted lactones, and this is further confirmed by the ROP of  $\delta$ -CL and  $\delta$ -DL with (thio)urea/IMes pairs, where the TOF values were up to  $996\text{ h}^{-1}$  and  $331\text{ h}^{-1}$ , respectively. Unlike previous ROPs of LA and unsubstituted lactones, the cooperative mechanism showed hardly any activity in the ROPs of omega-substituted lactones. In addition to the catalytic mechanism, steric hindrance induced by the substituents of the omega-substituted lactones also has a great impact on the polymerization activity. By changing the structure of thiourea from TU3 to TU4 with greater steric hindrance, the catalytic activity was significantly reduced with a TOF of only  $12\text{ h}^{-1}$ . Moreover, by utilizing the selectivity differences of different catalyst systems for the copolymerization of  $\epsilon$ -CL and  $\epsilon$ -DL, it is feasible to modulate the chain structure of the copolymers to easily achieve block, gradient and random structures. The modulation of monomer sequences during copolymerization is of great importance in polymer synthesis, as it significantly affects thermal and mechanical properties, allowing the construction of materials suitable for different applications. Besides, this polyester is promising for applications in the adhesive, coating, and biomedical fields. The above results provide ideas for the design of similar H-bond donor/acceptor catalysts and contribute to the development of more structurally diverse polymers.

## Author contributions

Jiang, Du and Zhu conceived the idea, proposed the strategy, designed the experiments, evaluated the data and wrote the manuscript together. Jiang performed the majority of the experiments. Liang, Wang, Qiang and Li participated in the polymerization experiments and related characterization analysis. All the authors proofread the manuscript.

## Conflicts of interest

There are no conflicts to declare.

## Acknowledgements

This work was supported by the National Key R&D Program of China (2022YFC2402900), the National Natural Science Foundation of China (51903190, 22175131, 22335005, and 21925505), the Innovation Program of Shanghai Municipal Education Commission (2023ZKZD28), and the International Scientific Collaboration Fund of Science and Technology Commission of Shanghai Municipality (21520710100). J. D. is a recipient of the National Science Fund for Distinguished Young Scholars.

## References

- 1 N. E. Kamber, W. Jeong, R. M. Waymouth, R. C. Pratt, B. G. G. Lohmeijer and J. L. Hedrick, *Chem. Rev.*, 2007, **107**, 5813–5840.
- 2 A.-C. Albertsson and I. K. Varma, *Biomacromolecules*, 2003, **4**, 1466–1486.
- 3 M. K. Kiesewetter, E. J. Shin, J. L. Hedrick and R. M. Waymouth, *Macromolecules*, 2010, **43**, 2093–2107.
- 4 A. Tardy, J. Nicolas, D. Gimes, C. Lefay and Y. Guillemeuf, *Chem. Rev.*, 2017, **117**, 1319–1406.
- 5 C. A. R. Picken, O. Buensoz, P. D. Price, C. Fidge, L. Points and M. P. Shaver, *Chem. Sci.*, 2023, **14**, 12926–12940.
- 6 W. Lu, J. E. Ness, W. Xie, X. Zhang, J. Minshull and R. A. Gross, *J. Am. Chem. Soc.*, 2010, **132**, 15451–15455.
- 7 R. Kourist and L. Hilterhaus, in *Microorganisms in Biorefineries*, ed. B. Kamm, Springer, Berlin, Heidelberg, 2015, vol. 26, pp. 275–301.
- 8 S. Katsuhara, Y. Takagi, N. Sunagawa, K. Igarashi, T. Yamamoto, K. Tajima, T. Isono and T. Satoh, *ACS Sustainable Chem. Eng.*, 2021, **9**, 9779–9788.
- 9 M. T. Martello, A. Burns and M. Hillmyer, *ACS Macro Lett.*, 2012, **1**, 131–135.
- 10 D. Bandelli, C. Helbing, C. Weber, M. Seifert, I. Muljajew, K. D. Jandt and U. S. Schubert, *Macromolecules*, 2018, **51**, 5567–5576.
- 11 C. Li, L. Wang, Q. Yan, F. Liu, Y. Shen and Z. Li, *Angew. Chem., Int. Ed.*, 2022, **61**, e202201407.



- 12 Q. Yan, C. Li, T. Yan, Y. Shen and Z. Li, *Macromolecules*, 2022, **55**, 3860–3868.
- 13 D. Bandelli, C. Weber and U. S. Schubert, *Macromol. Rapid Commun.*, 2019, **40**, 1900306.
- 14 J. R. Lowe, M. T. Martello, W. B. Tolman and M. A. Hillmyer, *Polym. Chem.*, 2011, **2**, 702–708.
- 15 D. Zhang, M. A. Hillmyer and W. B. Tolman, *Biomacromolecules*, 2005, **6**, 2091–2095.
- 16 J. A. Wilson, S. A. Hopkins, P. M. Wright and A. P. Dove, *Biomacromolecules*, 2015, **16**, 3191–3200.
- 17 G. L. Gregory, G. S. Sulley, L. P. Carrodeguas, T. T. D. Chen, A. Santmarti, N. J. Terrill, K.-Y. Lee and C. K. Williams, *Chem. Sci.*, 2020, **11**, 6567–6581.
- 18 S. Thongkham, J. Monot, B. Martin-Vaca and D. Bourissou, *Macromolecules*, 2019, **52**, 8103–8113.
- 19 C. Romain, Y. Zhu, P. Dingwall, S. Paul, H. S. Rzepa, A. Buchard and C. K. Williams, *J. Am. Chem. Soc.*, 2016, **138**, 4120–4131.
- 20 J.-F. Lutz, M. Ouchi, D. R. Liu and M. Sawamoto, *Science*, 2013, **341**, 1238149.
- 21 S. Rupf, P. Pröhm and A. J. Plajer, *Chem. Sci.*, 2022, **13**, 6355–6365.
- 22 R. C. Jeske, J. M. Rowley and G. W. Coates, *Angew. Chem., Int. Ed.*, 2008, **47**, 6041–6044.
- 23 C. Romain and C. K. Williams, *Angew. Chem., Int. Ed.*, 2014, **53**, 1607–1610.
- 24 Z. Yang, C. Hu, F. Cui, X. Pang, Y. Huang, Y. Zhou and X. Chen, *Angew. Chem., Int. Ed.*, 2022, **61**, e202117533.
- 25 V. K. Chidara, S. K. Boopathi, N. Hadjichristidis, Y. Gnanou and X. S. Feng, *Macromolecules*, 2021, **54**, 2711–2719.
- 26 J. B. Zhang, L. B. Wang, S. F. Liu, X. H. Kang and Z. B. Li, *Macromolecules*, 2021, **54**, 763–772.
- 27 Y. K. Ma, X. X. You, J. B. Zhang, X. W. Wang, X. H. Kou, S. F. Liu, R. L. Zhong and Z. B. Li, *Angew. Chem., Int. Ed.*, 2023, **62**, e202303315.
- 28 M. Hong, J. Chen and E. Y. X. Chen, *Chem. Rev.*, 2018, **118**, 10551–10616.
- 29 A. P. Dove, *ACS Macro Lett.*, 2012, **1**, 1409–1412.
- 30 B. Lin and R. M. Waymouth, *J. Am. Chem. Soc.*, 2017, **139**, 1645–1652.
- 31 K. V. Fastnacht, S. S. Spink, N. U. Dharmaratne, J. U. Pothupitiya, P. P. Datta, E. T. Kiesewetter and M. K. Kiesewetter, *ACS Macro Lett.*, 2016, **5**, 982–986.
- 32 X. Zhang, G. O. Jones, J. L. Hedrick and R. M. Waymouth, *Nat. Chem.*, 2016, **8**, 1047–1053.
- 33 J. U. Pothupitiya, R. S. Hewawasam and M. K. Kiesewetter, *Macromolecules*, 2018, **51**, 3203–3211.
- 34 P. Olsén, T. Borke, K. Odelius and A.-C. Albertsson, *Biomacromolecules*, 2013, **14**, 2883–2890.
- 35 L. Jasinska-Walc, M. Bouyahyi, A. Rozanski, R. Graf, M. R. Hansen and R. Duchateau, *Macromolecules*, 2015, **48**, 502–510.
- 36 J.-O. Lin, W. Chen, Z. Shen and J. Ling, *Macromolecules*, 2013, **46**, 7769–7776.
- 37 J. Bai, J. Wang, Y. Wang and L. Zhang, *Polym. Chem.*, 2018, **9**, 4875–4881.
- 38 B. Lin and R. M. Waymouth, *Macromolecules*, 2018, **51**, 2932–2938.
- 39 C. Romero-Guido, I. Belo, T. M. N. Ta, L. Cao-Hoang, M. Alchihab, N. Gomes, P. Thonart, J. A. Teixeira, J. Destain and Y. Waché, *Appl. Microbiol. Biotechnol.*, 2011, **89**, 535–547.
- 40 T. H. Parliment, W. W. Nawar and I. S. Fagerson, *J. Dairy Sci.*, 1965, **48**, 615–616.
- 41 T. Rali, S. W. Wossa and D. N. Leach, *Molecules*, 2007, **12**, 149–154.
- 42 G. Jakab, C. Tancon, Z. Zhang, K. M. Lippert and P. R. Schreiner, *Org. Lett.*, 2012, **14**, 1724–1727.
- 43 T. Bug, T. Lemek and H. Mayr, *J. Org. Chem.*, 2004, **69**, 7565–7576.
- 44 D. Martin, O. Illa, A. Baceiredo, G. Bertrand, R. M. Ortuño and V. Branchadell, *J. Org. Chem.*, 2005, **70**, 5671–5677.
- 45 R. Schwesinger, H. Schlemper, C. Hasenfratz, J. Willaredt, T. Dambacher, T. Breuer, C. Ottaway, M. Flentschinger, J. Boele, H. Fritz, D. Putzas, H. W. Rotter, F. G. Bordwell, A. V. Satish, G. Z. Ji, E. M. Peters, K. Peters, H. G. vonSchnering and L. Walz, *Liebigs Ann.*, 1996, 1055–1081.
- 46 R. M. Cywar, J.-B. Zhu and E. Y. X. Chen, *Polym. Chem.*, 2019, **10**, 3097–3106.
- 47 D. E. Gomez, L. Fabbriizzi, M. Licchelli and E. Monzani, *Org. Biomol. Chem.*, 2005, **3**, 1495–1500.
- 48 C. Perez-Casas and A. K. Yatsimirsky, *J. Org. Chem.*, 2008, **73**, 2275–2284.
- 49 G. Hua, J. Franzén and K. Odelius, *Polym. Chem.*, 2016, **54**, 1908–1918.
- 50 S. Penczek, *Polym. Chem.*, 2000, **38**, 1919–1933.
- 51 R. R. Walvoord, P. N. H. Huynh and M. C. Kozlowski, *J. Am. Chem. Soc.*, 2014, **136**, 16055–16065.
- 52 J. Ho, V. E. Zwicker, K. K. Y. Yuen and K. A. Jolliffe, *J. Org. Chem.*, 2017, **82**, 10732–10736.
- 53 M. R. Stühler, C. Gallizioli, S. M. Rupf and A. J. Plajer, *Polym. Chem.*, 2023, **14**, 4848–4855.
- 54 D. K. Schneiderman and M. A. Hillmyer, *Macromolecules*, 2016, **49**, 2419–2428.
- 55 P. Olsén, K. Odelius and A.-C. Albertsson, *Biomacromolecules*, 2016, **17**, 699–709.
- 56 J. Zhao and N. Hadjichristidis, *Polym. Chem.*, 2015, **6**, 2659–2668.
- 57 D. Bandelli, I. Muljajew, K. Scheuer, J. B. Max, C. Weber, F. H. Schacher, K. D. Jandt and U. S. Schubert, *Macromolecules*, 2020, **53**, 5208–5217.
- 58 H. Chen, R. Liu, S. Cai, Y. Zhang, C. Zhu, H. Yu and S. Li, *Biotechnol. J.*, 2024, **19**, e2300210.

